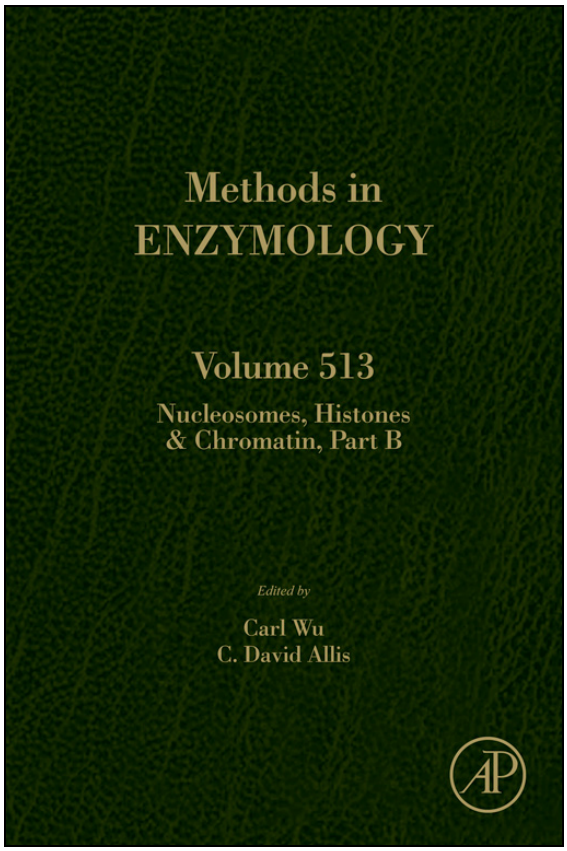
Provided for non-commercial research and educational use only.
Not for reproduction, distribution or commercial use.

This chapter was originally published in the book *Methods in Enzymology*, Vol. 513 published by Elsevier, and the attached copy is provided by Elsevier for the author's benefit and for the benefit of the author's institution, for non-commercial research and educational use including without limitation use in instruction at your institution, sending it to specific colleagues who know you, and providing a copy to your institution's administrator.



All other uses, reproduction and distribution, including without limitation commercial reprints, selling or licensing copies or access, or posting on open internet sites, your personal or institution's website or repository, are prohibited. For exceptions, permission may be sought for such use through Elsevier's permissions site at:
http://www.elsevier.com/locate/permissionusematerial

From: Ming Li and Michelle D. Wang, Unzipping Single DNA Molecules to Study Nucleosome Structure and Dynamics. In Carl Wu and C. David Allis, editors: Methods in Enzymology, Vol. 513, Burlington: Academic Press, 2012, pp. 29-58.
ISBN: 978-0-12-391938-0
© Copyright 2012 Elsevier Inc.
Academic Press

Author's personal copy

CHAPTER TWO

Unzipping Single DNA Molecules to Study Nucleosome Structure and Dynamics

Ming Li*, Michelle D. Wang[†,‡,1]

*Department of Chemistry and Chemical Biology, Cornell University, Ithaca, New York, USA
[†]Department of Physics, Laboratory of Atomic and Solid State Physics, Cornell University, Ithaca, New York, USA
[‡]Howard Hughes Medical Institute, Cornell University, Ithaca, New York, USA
[1]Corresponding author: e-mail address: mwang@physics.cornell.edu

Contents

1. Introduction 30
2. Sample Preparation 33
   2.1 DNA unzipping template design 33
   2.2 Nucleosome reconstitution 36
   2.3 Formation of the final unzipping template 37
   2.4 Preparation of experimental sample chambers 38
3. Instrumentation and Data Collection 39
   3.1 Layout of single-beam optical trapping apparatus 39
   3.2 Calibration of the optical trapping system 41
   3.3 Experimental control: loading rate clamp and force clamp 41
   3.4 Data acquisition 42
4. Data Processing 43
   4.1 DNA elastic parameter determination 43
   4.2 Trap height determination for individual unzipping curves 43
   4.3 Data conversion to force and extension based on geometry 44
   4.4 Conversion to number of base pairs unzipped (j) 44
   4.5 Unzipping curve alignment 45
5. Determination of Unzipping Accuracy and Precision 46
6. Unzipping in Nucleosome Studies 48
   6.1 Nucleosome unzipping signature 48
   6.2 High-resolution mapping of histone–DNA interactions in a nucleosome 50
   6.3 Nucleosome remodeling 54
7. Conclusions 56
Acknowledgments 56
References 56

Methods in Enzymology, Volume 513
ISSN 0076-6879
http://dx.doi.org/10.1016/B978-0-12-391938-0.00002-1

© 2012 Elsevier Inc.
All rights reserved.

Author's personal copy

Abstract

DNA unzipping is a powerful tool to study protein–DNA interactions at the single-molecule level. In this chapter, we provide a detailed and practical guide to performing this technique with an optical trap, using nucleosome studies as an example. We detail protocols for preparing an unzipping template, constructing and calibrating the instrument, and acquiring, processing, and analyzing unzipping data. We also summarize major results from utilization of this technique for the studies of nucleosome structure, dynamics, positioning, and remodeling.

1. INTRODUCTION

As the fundamental units of eukaryotic chromatin, nucleosomes are responsible for packaging the genome into the nucleus and regulating access to genetic information during various cellular processes. The nucleosome core particle consists of 147 bp of DNA wrapped ~1.7 times around a histone octamer, containing two copies of H2A, H2B, H3, and H4 (Luger, Mader, Richmond, Sargent, & Richmond, 1997). The nonuniform distribution of histone–DNA interactions within a nucleosome governs its dynamic role in regulating access to nucleosomal DNA during transcription, replication, and DNA repair (Andrews & Luger, 2011; Korber & Becker, 2010). The position of nucleosomes along the genome is not only influenced by the properties of the underlying DNA sequence (Kaplan et al., 2009) but is also regulated by various histone chaperones (Das, Tyler, & Churchill, 2010; Park & Luger, 2008; Ransom, Dennehey, & Tyler, 2010), ATP-dependent chromatin remodeling complexes (Bowman, 2010; Clapier & Cairns, 2009), and other DNA-binding proteins, such as transcription factors (Bell, Tiwari, Thoma, & Schubeler, 2011; Zhang et al., 2009). In addition, several types of epigenetic marks, including covalent histone modifications, affect both the structure and stability of nucleosomes, as well as higher-order chromatin structure (Bannister & Kouzarides, 2011; Campos & Reinberg, 2009; Ray-Gallet & Almouzni, 2010). Thus, a detailed understanding of nucleosome structure and dynamics, as well as the relationship between nucleosomes and relevant regulatory factors, is of great interest to multiple fields and can enhance our knowledge of the basic tenets of biology.

Single-molecule techniques offer the unique ability to both detect the inherent heterogeneities of biomolecules and directly monitor dynamic

Author's personal copy

processes in real time and are thus important complementary to ensemble studies for understanding various biological systems (Joo, Balci, Ishitsuka, Buranachai, & Ha, 2008; Killian, Li, Sheinin, & Wang, 2012; Moffitt, Chemla, Smith, & Bustamante, 2008). In particular, DNA stretching experiments utilizing single-molecule manipulation techniques, such as magnetic tweezers or optical tweezers, allow for the direct investigation of the mechanical properties of both single nucleosomes and nucleosome arrays (Brower-Toland et al., 2002; Gemmen et al., 2005; Mihardja, Spakowitz, Zhang, & Bustamante, 2006; Simon et al., 2011). However, stretching experiments are unable to directly determine the location of a nucleosome on a long DNA template or directly probe the absolute locations of specific histone–DNA interactions in a nucleosome. To overcome these limitations, we developed an optical trapping-based single-molecule unzipping technique as a versatile tool to probe a variety of protein–DNA interactions (Dechassa et al., 2011; Hall et al., 2009; Jiang et al., 2005; Jin et al., 2010; Koch, Shundrovsky, Jantzen, & Wang, 2002; Koch & Wang, 2003; Shundrovsky, Smith, Lis, Peterson, & Wang, 2006). The unzipping technique is a straightforward concept and may be incorporated into different optical trapping configurations (an example is shown in Fig. 2.1). Briefly, a single double-stranded DNA (dsDNA) is unzipped in the presence of DNA-binding proteins. Mechanical force is applied to separate dsDNA into two single strands (Fig. 2.1A). DNA-bound proteins or protein complexes act as barriers to the unzipping fork so that resistance to unzipping provides a measure of the strengths of protein–DNA interactions, while the amount of DNA unzipped reveals the locations of these interactions along the DNA. These locations may be mapped to near base-pair precision and accuracy, making unzipping a powerful high-resolution technique for mapping these interactions.

Unzipping is a unique and extremely powerful single-molecule technique with many advantages: (1) The interaction map of a protein–DNA complex, as characterized by the strengths and locations of interactions, provides important structural information about the complex (Dechassa et al., 2011; Hall et al., 2009; Jin et al., 2010; Shundrovsky et al., 2006); (2) The footprint of a bound complex can be directly measured by unzipping DNA molecules from both directions (Dechassa et al., 2011; Hall et al., 2009; Jiang et al., 2005; Jin et al., 2010); (3) Unzipping directly reveals the presence or absence of a bound protein, making it an ideal method for measuring its equilibrium dissociation constant, even for tight binding in the pM range (Jiang et al., 2005; Koch et al., 2002); (4) Using dynamic force

Author's personal copy

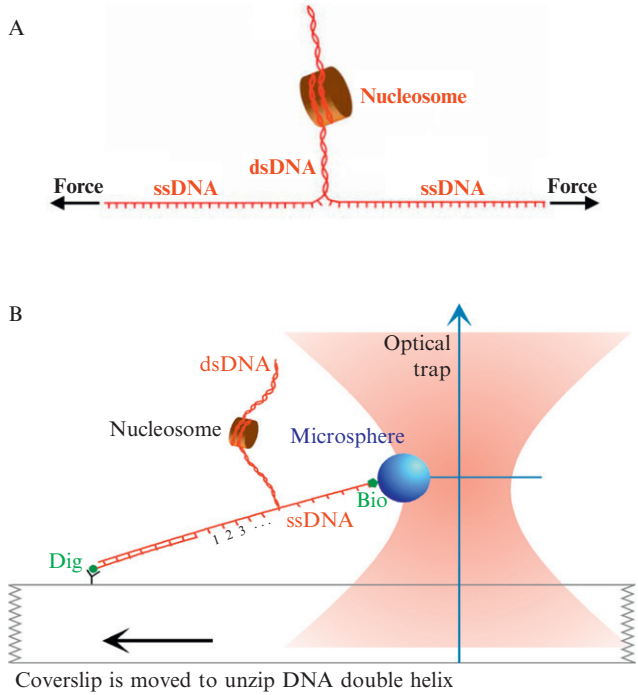


Figure 2.1 Experimental unzipping configuration. (Adapted from Hall et al., 2009 and Shundrovsky et al., 2006, with permissions from the publishers.) (A) A simplified cartoon of the unzipping configuration. A DNA double helix is mechanically unzipped in the presence of DNA-binding proteins, such as a nucleosome, by the application of opposing forces on the two strands. (B) A typical experimental configuration for unzipping. An optical trap is used to apply a force necessary to unzip through the DNA as the coverslip is moved away from the trapped microsphere.

measurements, it is possible to differentiate different bound species which may bind to the same DNA sequence (Koch & Wang, 2003); (5) Unzipping is capable of determining the location of a protein on a very long DNA molecule with near base-pair accuracy, making it ideal for studying the positioning and/or repositioning of proteins and protein complexes along DNA (Shundrovsky et al., 2006).

Unzipping has been successfully utilized to study the binding affinity of restriction enzymes (Koch et al., 2002; Koch & Wang, 2003), mismatch detection by DNA repair enzymes (Jiang et al., 2005), the dynamics of nucleosome structure and positioning (Dechassa et al., 2011; Hall et al., 2009; Shundrovsky et al., 2006), and how RNA polymerase overcomes a

Author's personal copy

nucleosome barrier (Jin et al., 2010). For clarity and brevity, we focus below on the experimental procedures utilizing our particular single-beam optical trapping system to study nucleosome structure and dynamics (Fig. 2.1B).

2. SAMPLE PREPARATION

2.1. DNA unzipping template design

Here, we detail the construction of unzipping templates that can be used with the optical trapping system shown in Fig. 2.1B. Although different experimental configurations may require somewhat different templates, the general template designs share common features (Bockelmann, Essevaz-Roulet, & Heslot, 1998; Koch et al., 2002). The template generally consists of two segments: an anchoring segment and an unzipping segment, separated by a nick (Fig. 2.2). At one end of the anchoring segment is a tag that will bind to the coverslip, and near the nick is a different tag that will bind to a microsphere. By moving the coverslip away from the trapped microsphere, the unzipping segment can be unzipped.

The anchoring segment is generally 1–2 kb long and consists of a dsDNA linker arm with an end-labeled digoxigenin tag. This length will provide sufficient distance between the anchor point and the unzipping segment to ensure that the trapped microsphere does not contact the coverslip surface. This will facilitate data analysis. However, an anchoring segment that is too long will lead to increased Brownian noise of the trapped microsphere and compromise the accuracy of position measurements.

The unzipping segment consists of an experiment-specific target sequence with an internal biotin tag near the nick. This segment may also contain bound proteins or protein complexes to be studied. The length of the unzipping segment can vary from hundreds to a few thousands of base pairs. Note that a segment that is too short will not allow for optimal data alignment (detailed in a later section). Bound proteins or protein complexes can be located in any region of the unzipping segment, although we typically leave at least 200 bp of flanking DNA on either side of a bound protein to ensure accuracy during data alignment. In some experiments, unzipping should be conducted from both directions (forward and reverse) along the same unzipping segment to investigate possible asymmetric binding. Therefore, both forward and reverse unzipping segments should be prepared.

As an example, we provide below a detailed protocol for constructing a typical forward unzipping template for studying histone–DNA interactions

Author's personal copy

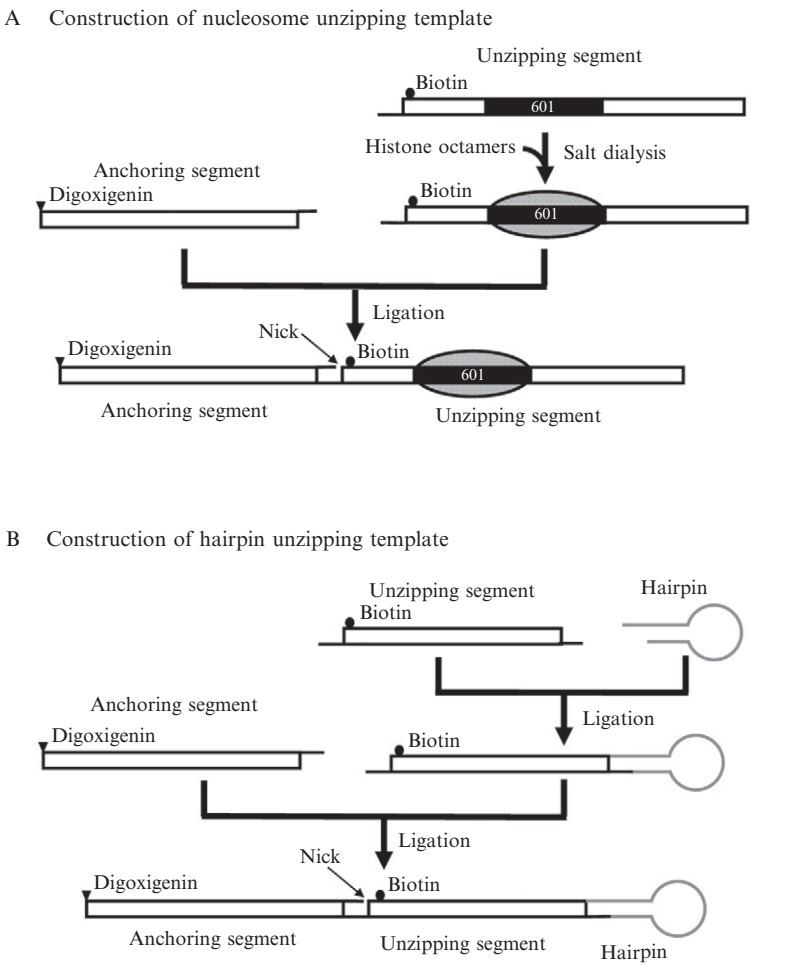


Figure 2.2 Unzipping template construction. (A) Construction of a nucleosome unzipping template. A DNA template for nucleosome unzipping experiments consists of a digoxigenin-labeled anchoring segment and a biotin-labeled nucleosome unzipping segment. As an example, a nucleosome unzipping segment is shown containing a 601 nucleosome positioning sequence. (B) Construction of a hairpin-capped unzipping template. This template consists of a digoxigenin-labeled anchoring segment and a biotin-labeled unzipping segment with a hairpin capped at the distal end.

in a single nucleosome (Dechassa et al., 2011; Hall et al., 2009; Shundrovsky et al., 2006). In this template, the anchoring segment is 1.1 kb and the unzipping segment is 774 bp. The nucleosome is located near the center of the unzipping template and is well positioned on a 147-bp "Widom 601" nucleosome positioning element (601), which has an extremely

Author's personal copy

high affinity for a nucleosome (Fig. 2.2) (Lowary & Widom, 1998). Labeling and producing the DNA templates are accomplished by standard enzymatic reactions and purification methods with biotin and digoxigenin-labeled nucleic acids. These two labels are especially convenient due to the ease of covalent attachment of streptavidin (Sigma) to carboxylated polystyrene microspheres (Polysciences, Inc.) and the availability of high-affinity antidigoxigenin antibodies (Roche Applied Sciences, Indianapolis, IN). The reverse nucleosomal unzipping segment is prepared using methods nearly identical to those of the forward unzipping segment, except that the entire segment is flipped by the use of different primers, such that the ligatable overhang is located on the opposite end.

Anchoring segment preparation

1. PCR amplify the anchoring segment from plasmid pRL574 (Schafer, Gelles, Sheetz, & Landick, 1991). The forward primer contains a 5′-digoxigenin label, designed to be ~1.1 kb away from the single BstXI cutting site located on the plasmid.
2. BstXI (New England Biolabs) digest the PCR product to generate a 3′-overhang for ligation of the unzipping segment.

Unzipping segment preparation

1. PCR amplify the unzipping segment from plasmid p601 (Lowary & Widom, 1998). The forward primer was designed to be ~200 bp upstream of the 601 element and to contain a BstXI cutting site. This site will be utilized to generate a 3′-overhang complementary to the one produced on the anchoring segment. The forward primer contains an internal biotin label near the 3′-overhang. The reverse primer is located ~400 bp downstream of the 601 element.
2. BstXI (New England Biolabs) digest the PCR product. Follow the digestion with the addition of a stoichiometric amount of calf intestinal alkaline phosphatase (CIP, New England Biolabs) in the same buffer, to remove the phosphate from the 3′-overhang. This allows for the generation of a nick after subsequent ligation (discussed below in Section 2.3).

To characterize the precision and accuracy of the unzipping method in locating a bound protein along the DNA (discussed later), we have also designed multiple unzipping templates of varying lengths, capped with hairpins at distal ends (Fig. 2.2B). These hairpins act as strong binding sites by preventing further unzipping at well-defined locations along the DNA and allow for a direction comparison with measured locations. In addition, these unzipping templates are also used to determine the elastic parameters of

Author's personal copy

single-stranded DNA (ssDNA) under experimental conditions discussed below. Here, we have outlined a protocol for constructing hairpin-capped unzipping segments of various lengths.

1. PCR amplify the unzipping segment from p601 using the same forward primer specified above in "unzipping segment preparation." The reverse primers are located at various distances downstream from the forward primer to generate templates of different lengths. The reverse primer is also designed to contain an EarI cutting site that will generate a 5′-overhang.
2. EarI (New England Biolabs) digest the PCR products to generate a 5′-overhang.
3. The oligonucleotide (Integrated DNA Technologies) utilized to generate the hairpin is designed to form a three-base hairpin loop and a short dsDNA stem (~12 bp) with a 5′-overhang which is complementary to the overhang in the unzipping segment.
4. Ligate the unzipping segment with a hairpin oligonucleotide (1:10 molar ratio) using T4 Ligase (New England Biolabs). Overnight ligation is normally necessary to maximize the ligation yield. Purify the ligated products using agarose gel purification.
5. BstXI (New England Biolabs) digest the gel purified product to generate an overhang near the biotin label. Following the digestion, add a stoichiometric amount of CIP (New England Biolabs) in the same digestion buffer to remove the phosphate from the 3′-overhang. This allows for the generation of a nick after ligation with the anchoring segment (discussed below in Section 2.3).

2.2. Nucleosome reconstitution

It has been well established that *in vitro* assembly of nucleosomes and chromatin arrays from highly purified DNA and histone components can be achieved by either salt-gradient dialysis (Luger, Rechsteiner, & Richmond, 1999) or a chaperone-mediated approach (Fyodorov & Kadonaga, 2003). We employ a salt-gradient dialysis method for nucleosome reconstitution. Different types of individual histones can be prepared as previously described (Dyer et al., 2004). Purified histone octamers from several species are also commercially available in forms suitable for reconstitution (Protein Expression/Purification Facility, Colorado State University). In our previous publications (Dechassa et al., 2011; Hall et al., 2009; Jin et al., 2010;

Author's personal copy

Shundrovsky et al., 2006), a well-established salt dialysis method (Dyer et al., 2004; Thastrom, Lowary, & Widom, 2004) was modified to reconstitute a single nucleosome on a long piece of DNA containing one 601 positioning element. The modified protocol uses a small total volume and requires a low concentration of DNA template and histones (100 n*M* or even lower) that are suitable for single-molecule studies. The modifications are listed below.

1. The dialysis button is constructed following the procedure from Thastrom et al. (2004). This allows us to work with assembly volumes of ~30 μL, which is much smaller than commercially available dialysis chambers.
2. We include 0.2 g/L sodium azide (Sigma-Aldrich) in both the high and low salt buffers to remove bacteria which may contaminate the buffers and decrease assembly efficiency.
3. We include 0.1 mg/mL acetylated BSA (acBSA) (Ambion) to each dialysis button as a crowding agent to assist with assembly.
4. The dialysis is performed at 4 °C and the dialysis pump is set to 1.2 mL/min for ~18 h. The flow is then changed to 2.5 mL/min for an additional ~4 h.
5. After dialysis, the samples are transferred to zero salt buffer and incubated for 2–3 h at 4 °C.

Fine-tuning the molar ratio between the histone octamer and DNA template is critical to achieve a high reconstitution yield and avoid over assembly. In addition, it is also important to remove bubbles from the dialysis button, because bubbles can prevent buffer exchange between the high salt solution and the sample. After reconstitution, the nucleosome samples may be stored for a few weeks at 4 °C.

2.3. Formation of the final unzipping template

The unzipping segment (containing either a nucleosome or a hairpin) is directly ligated to the anchoring segment (in a 1:1 molar ratio) immediately prior to use (Fig. 2.2). The CIP dephosphorylation of the unzipping segment ensures that only one strand of the DNA is ligated and a nick is generated on the complementary strand during the ligation step. This complete unzipping template is labeled with a single digoxigenin tag at the 5′-end of the anchor segment and a biotin tag located near the nick on the unzipping segment. A complete template lacking a nucleosome (naked DNA) is stable for a few days without DNA nicking at 4 °C; a template containing a nucleosome should be used within a few hours of ligation.

Author's personal copy

2.4. Preparation of experimental sample chambers

For single-molecule studies in general, individual DNA tethers need to be immobilized in a single-molecule sample chamber or a flow cell. These allow the user to sequentially flow in different solutions for use with the optical trapping system. In our nucleosome unzipping studies, sample chambers with an ~15 μL volume are prepared at room temperature and then mounted onto an optical trapping setup. By performing incubations in a humid chamber prior to mounting onto the optical setup, buffer evaporation can be minimized.

Buffer solutions

1. Sample buffer (SB): 10 m*M* Tris HCl (pH 7.5), 1 m*M* Na_2EDTA, 150 m*M* NaCl, 3% (v/v) glycerol, 1 m*M* DTT, 0.1 mg/mL acBSA.
2. Blocking buffer (BB): SB + 5 mg/mL casein sodium salt from bovine milk.
3. Nucleosome unzipping buffer (NUB): 10 m*M* Tris HCl (pH 8.0), 1 m*M* Na_2EDTA, 100 m*M* NaCl, 1.5 m*M* $MgCl_2$, 3% (v/v) glyercol, 1 m*M* DTT, 0.02% (v/v) Tween20, 2 mg/mL acBSA.

Blocking agents are used to coat the surface of the sample chamber to prevent unwanted protein attachment to the surface. The blocking agent that has been the most successful for us is casein sodium salt from bovine milk (Sigma-Aldrich Co.). AcBSA is thought to mimic conditions of a higher protein concentration in the sample buffer, creating a more "crowded" environment, and thus prevents protein dissociation from the template (Gansen, Hauger, Toth, & Langowski, 2007). We utilize a polyclonal sheep antidigoxigenin (Roche Applied Sciences) for attachment of digoxigenin-labeled DNA samples to sample chamber surfaces. The complete unzipping template is diluted to a desired concentration in SB immediately before introduction to sample chamber. The detailed procedure of creating a tethered DNA sample chamber is given below:

1. Apply two thin pieces of double-stick tape (~0.1 mm thick) to a coverslip (24 mm × 40 mm × 0.15 mm). Orient the pieces parallel to one another and separate them by ~5 mm.
2. Place a glass slide on top of the coverslip and perpendicular to it, to create an ~15-μL channel down the center.
3. Flow in one volume (~15 μL) of antidigoxigenin solution (20 ng/μL in H_2O).
4. Incubate for 5 min. Wash with five volumes of BB. Incubate with residual blocker for 5 min.
5. Wash with five volumes of SB. Immediately flow in one volume of diluted unzipping template in SB. Incubate for 10 min.

Author's personal copy

6. Wash with five volumes of SB. Flow in one volume of streptavidin-coated polystyrene microspheres (5 p*M* in BB). Incubate for 10 min.
7. Wash with 10 volumes of NUB.

The concentration to which the unzipping sample is diluted prior to being added to the sample chamber is critical for achieving an optimal tether density under single-molecule conditions. A concentration that is too high will lead to multiple tethers (one microsphere attached to multiple DNA molecules) and a concentration that is too low will make it difficult to locate a suitable unzipping tether. In theory, 10 p*M* of DNA template is needed to achieve an acceptable tether density. However, as the ligated templates are directly diluted without purification, the appropriate "flow-in" concentration depends heavily on the ligation efficiency. Therefore, for each new template, several chambers with different template concentrations are often made and evaluated to establish an appropriate flow-in concentration.

Consistency in all aspects of sample preparation and utilization is critical to achieve reproducible results among different sample chambers. In this regard, unzipping experiments are conducted in a temperature- and humidity-controlled soundproof room. Once prepared, the sample chambers should be utilized in a timely fashion, typically within 1 h, to avoid unnecessary complications such as protein dissociation or sample sticking to the surface of the chamber.

3. INSTRUMENTATION AND DATA COLLECTION

3.1. Layout of single-beam optical trapping apparatus

Since the pioneering work by Arthur Ashkin over 20 years ago (Ashkin, Dziedzic, Bjorkholm, & Chu, 1986), the optical trapping field has grown tremendously due to the unique ability of optical tweezers to monitor and manipulate biological targets with high temporal and spatial resolution. In addition, refinements of established methods and the integration of this tool with other forms of single-molecule manipulation or detection have made this technique of great interest in both physics and biology. The single-beam optical trapping instrument that we use has a very straightforward design (Brower-Toland & Wang, 2004; Koch et al., 2002), containing the minimal set of optical components required for the operation of a high-precision instrument of its kind (Fig. 2.3). A 1064-nm laser (Spectra-Physics Lasers, Inc. Mountain View, CA) is transmitted through

Author's personal copy

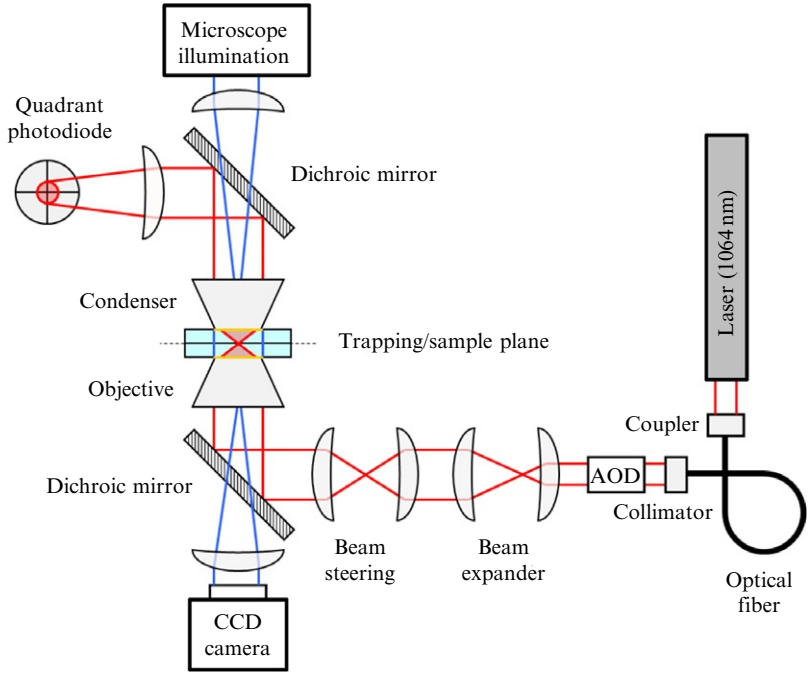


Figure 2.3 Layout of the optical trapping apparatus. See text for a detailed description of the setup.

a single-mode optical fiber (Oz Optics, Carp, ON), expanded by a telescope lens pair, and focused onto the back focal plane of a 100×, 1.4 NA oil-immersion microscope objective that is mounted in a modified Eclipse TE 200 DIC inverted microscope (Nikon USA, Melville, NY). The focused beam serves as a trap for a 500-nm polystyrene microsphere (Polysciences, Inc.). Forward-scattered light is collected by a condenser lens and imaged onto a quadrant photodiode (Hamamatsu, Bridgewater, NJ). A displacement of a trapped microsphere imparts a deflection of the forward-scattered light and is captured as a differential voltage signal at the quadrant photodiode. The laser intensity is adjusted by modulating the voltage amplitude applied to an acoustic optical deflector (AOD) (NEOS Technologies, Inc., Melbourne, FL) placed between the laser aperture and the beam expander. Samples are manipulated manually via a microstage or via a high-precision 3D piezoelectric stage (Mad City Labs, Madison, WI). Analog voltage signals from the position detector and

Author's personal copy

stage position sensor are anti-alias filtered at 5 kHz (Krohn-Hite, Avon, MA) and digitized at 7–13 kHz for each channel using a multiplexed analog to digital conversion PCIe board (National Instruments Corporation, Austin, TX).

3.2. Calibration of the optical trapping system

The instrument calibration methods for our optical trapping setup were detailed in a previous publication (Wang, Yin, Landick, Gelles, & Block, 1997). In brief, they include (1) the determination of the position detector sensitivity and the trap stiffness, (2) the determination of the position of the trap center relative to the beam waist and the height of the trap center relative to the coverslip, and (3) the location of the anchor position of the unzipping tether on the coverslip, which is determined prior to each measurement by stretching the anchoring segment laterally at a low load (<5 pN). These calibrations are subsequently used to convert raw data into force and extension values.

3.3. Experimental control: loading rate clamp and force clamp

In nucleosome unzipping experiments, we often use two approaches to disrupt a nucleosome: loading rate clamp unzipping and force clamp unzipping. The advantages and disadvantages of these two methods are discussed below.

A loading rate clamp allows the force to increase linearly at a specific rate until the disruption of an interaction. This approach generates distinct force unzipping signatures (unzipping force as a function of the number of base pair unzipped) which can be used to distinguish a nucleosome from other DNA-binding proteins. Because the disruption is a thermally activated process (Evans, 2001), the force needed to disrupt a specific interaction in the nucleosome is dependent on the loading rate as well as the starting force. After a disruption, the force naturally drops but is not allowed to recover to the naked DNA unzipping baseline. Consequently, the starting force for a subsequent disruption is higher than for the initial disruption. Thus, weak interactions in a nucleosome may be detected if they are first encountered by the unzipping fork. This method may be used to highlight weak histone–DNA interactions near the entrance and exit sites. It will of course detect all strong interactions.

A force clamp allows for the disruption of all interactions in a nucleosome under the same force. This is well suited to a quantitative analysis of the strength of the detected interactions (Forties et al., 2011). However,

Author's personal copy

more experimentation is normally required to determine an appropriate range of desired unzipping forces. A force that is too small will make the time to disrupt the nucleosome too long to be experimentally accessible, and a force that is too large may overlook specific interactions in the nucleosome. A force clamp is usually implemented with loading rate clamps before and after it to simplify data alignment (discussed further below). A loading rate clamp is most suitable to study the interactions around the periphery of a nucleosome, while the force-clamp mode is optimal for determining the interactions around the dyad. More importantly, a loading rate clamp provides a clear force unzipping signature, while a force clamp is more convenient in quantitative analysis of the energy landscape of histone–DNA interactions in a nucleosome.

3.4. Data acquisition

Here, we detail the process of data collection using the two aforementioned approaches.

When utilizing the loading rate clamp mode (Dechassa et al., 2011; Hall et al., 2009; Koch & Wang, 2003; Shundrovsky et al., 2006), the microscope coverslip velocity is adjusted to produce a constant force-loading rate by controlling the position of the piezo stage, while the position of the microsphere in the trap is kept constant by modulating the light intensity (trap stiffness) of the trapping laser. Unzipping through a nucleosome is visualized as a group of force peaks up to 30–40 pN ramping up linearly above the naked DNA unzipping baseline (13–16 pN). In the force-clamp mode (Hall et al., 2009), the unzipping begins with a loading rate clamp until the desired force (threshold force) is reached within a nucleosome. The unzipping force is then held constant via feedback control of the coverslip position. The threshold force is carefully selected so that it is much higher than the baseline unzipping force of the naked DNA, but is still low enough to allow sufficient dwell time at most histone–DNA interactions for detection. Upon passing through the nucleosome region, the unzipping reverts to the original loading rate clamp. The distinctive naked DNA unzipping signatures, detected by the loading rate clamp before and after the nucleosome, are important for data alignment (see below).

Apart from the two unzipping modes presented above, we can also modulate the unzipping process to allow the DNA to be unzipped and rezipped multiple times by controlling the unzipping forces and the corresponding position of the piezo stage. This modulation allows unzipping experiments

Author's personal copy

to potentially mimic important biological process, such as a motor protein progressing into a nucleosome (Hall et al., 2009).

4. DATA PROCESSING

Data acquired by the optical trapping setup need to be processed according to these steps: (1) determine the elastic parameters of the dsDNA and ssDNA, (2) determine trap height, (3) perform data conversion to force and extension based on geometry, (4) convert DNA extension to number of base pairs unzipped, (5) perform data alignment against a theoretical curve. These steps are detailed below.

4.1. DNA elastic parameter determination

As unzipping experiments involve the extension of dsDNA (the anchoring segment) in series with ssDNA (unzipped DNA) (Fig. 2.1B), elastic parameters of both dsDNA and ssDNA are necessary for data analysis. These parameters are strongly dependent on the buffer conditions used in unzipping experiments. We obtain elastic parameters of dsDNA by stretching dsDNA and fitting the resulting force versus extension curve to a modified worm-like chain model under the same buffer conditions as the actual unzipping experiment following the detailed procedures published previously (Wang et al., 1997). To obtain the elastic parameters of ssDNA, we unzip a template capped with a hairpin at the distal end under the same buffer conditions as the actual unzipping experiment (Koch et al., 2002; Hall et al., 2009). Once completely unzipped, the unzipped DNA is then stretched to a high force (up to 50 pN) to obtain the force-extension curve, which reflects elastic contributions from both the dsDNA and ssDNA. Given the elastic parameters of dsDNA under these conditions, this curve allows for the determination of the elastic properties of ssDNA using an extensible freely jointed chain (FJC) model (Smith et al., 1996).

4.2. Trap height determination for individual unzipping curves

Prior to nucleosome unzipping experiments, we calibrate the height of the trap center relative to the surface of the coverslip when the objective is focused on the coverslip surface (Wang et al., 1997); it is typically found to be $\sim$600 nm. However, the actual trap height during a nucleosome unzipping experiment may differ from the calibrated height by as much as 100 nm due to limited focusing precision. We have therefore implemented

Author's personal copy

a technique to obtain trace-specific trap height of the unzipping data. In this method, we analyze the initial segment of the data prior to strand separation (0–10 pN). Because DNA is not yet unzipped, the expected force-extension curve has been fully characterized as described in Section 4.1 and is simply that of the dsDNA anchoring segment of known contour length. The trap height is determined when the difference between the converted force-extension curve and the expected curve is minimized.

4.3. Data conversion to force and extension based on geometry

Once the trap height is determined, force and extension of DNA as a function of time may be obtained following a method that has been previously described in detail (Wang et al., 1997). At a given time point, a number of parameters must be detected and/or calibrated: DNA anchor point on the coverslip, the position of the trapped microsphere relative to the trap center, and the stiffness of the trap. The results of the conversion are the force (F) and extension (x) along the direction of the stretched DNA molecule.

4.4. Conversion to number of base pairs unzipped (j)

Once the unzipping data are converted to force (F) and extension (x) for a given time point (t), the number of base pairs unzipped (j) at each time point may be obtained. The extension of the DNA (x) contains contributions from both the dsDNA (x_{ds}) and ssDNA (x_{ss}) under the same force:

$$x(F) = x_{ds}(F) + x_{ss}(F) \tag{2.1}$$

$x_{ds}(F)$ is determined because the force-extension curve of the anchoring segment is fully characterized. $x_{ss}(F)$ is thus obtained from Eq. (2.1) and is proportional to the number of ssDNA nucleotides. Using the extensible FJC model, $x_{ss}(F)$ is converted to the number of base pairs unzipped (j).

As the DNA is extended but prior to strand separation, $j = 0$ bp, resulting in a vertical rise in the F versus j plot (Fig. 2.4A). Once strand separation starts, a characteristic force signature, determined by the underlying DNA sequence as discussed below, is detected with an increase in j. In the presence of bound proteins, this gently varying baseline is interrupted by sharp force rises. When the unzipping fork encounters a strong protein–DNA interaction, force increases linearly, while the number of base pair unzipped remains unchanged until the sudden dissociation of the bound protein, leading to a sudden reduction in the force. Therefore, the F versus j plot

Author's personal copy

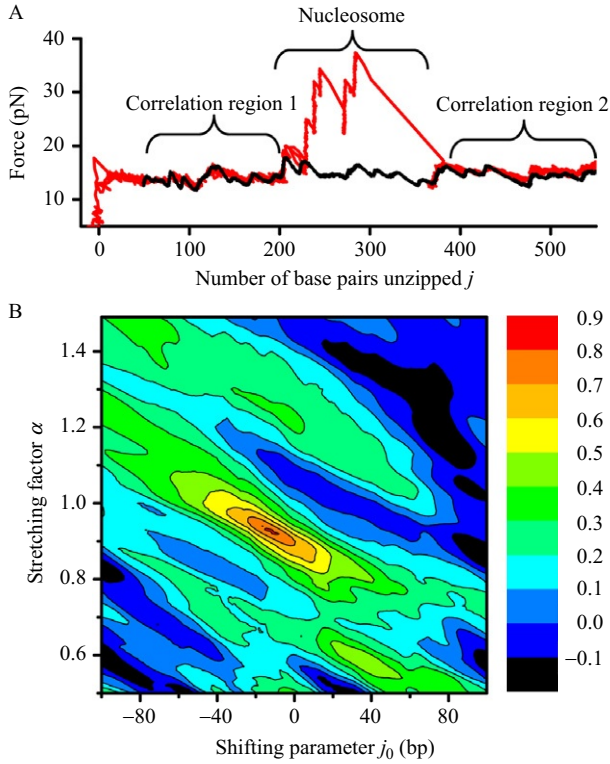


Figure 2.4 Unzipping curve alignment. (A) An example of force versus number of base pairs unzipped plot for a nucleosome unzipping curve (red) after alignment with the corresponding theoretical curve for naked DNA of the same sequence (black). Unzipping was carried out at a loading rate of 8 pN/s. Regions 1 and 2 flanking the nucleosome were used for correlation. Note also that the initial rise of force is located at $j = 0$ bp, corresponding to stretching of the anchoring segment before strand separation. (B) A two-dimensional intensity graph of the generalized correlation function $R(a, j_0)$ for the trace shown in A. The peak $R = 0.80$ is located at stretching factor $a = 0.93$ and shifting parameter $j = -14$ bp.

provides a direct measurement of (1) the location of the bound protein on the DNA (j at which the force rise starts) and (2) the strength of the interaction (force magnitude).

4.5. Unzipping curve alignment

Although the raw F versus j plot already contains critical information about a bound protein, the precision and accuracy of locating a bound protein are limited to $\sim$10 bp, due to small but significant uncertainties in a number of

Author's personal copy

parameters (trap height, microshpere size, and trapped microshpere position and force). In order to improve on this, we take advantage of the characteristic unzipping force signatures that depend strongly on the DNA sequence and align an experimental unzipping force curve $F_{\text{exp}}(j)$ against a theoretical curve $F_{\text{theo}}(j)$. $F_{\text{theo}}(j)$ is computed based on an equilibrium statistical mechanics model that considers sequence-dependent base pairing energy and DNA elasticity(Bockelmann et al., 1998). During the correlation, the argument of $F_{\text{exp}}(j)$ is both shifted by j_0 number of base pairs and stretched by a factor of a. The best values of j_0 and a are obtained by maximizing the following generalized cross-correlation function:

$$R(a,j_0)=\frac{\int \mathrm{d}j[F_{\text{theo}}(j)-\bar{F}_{\text{theo}}][F_{\text{exp}}(aj+j_0)-\bar{F}_{\text{exp}}]}{\sqrt{\int \mathrm{d}j[F_{\text{theo}}(j)-\bar{F}_{\text{theo}}]^2\int \mathrm{d}j[F_{\text{exp}}(aj+j_0)-\bar{F}_{\text{exp}}]^2}} \tag{2.2}$$

where $\bar{F}_{\text{theo}}$ and $\bar{F}_{\text{exp}}$ are the mean values of the $\bar{F}_{\text{theo}}(j)$ and $\bar{F}_{\text{exp}}(aj+j_0)$, respectively. The search for optimal j_0 and a may be also facilitated by the use of a SIMPLEX search algorithm.

When using this method to align a trace taken from DNA containing a nucleosome against the known DNA sequence, regions of naked DNA, $\sim$100–200 bp, adjacent to the nucleosome should be used for correlation. We found that once unzipping passes a nucleosome, the unzipping curve immediately following the nucleosome did not always show the expected naked DNA pattern (Shundrovsky et al., 2006). Instead, in some traces we observed random high-force peaks that were not present when unzipping naked DNA. We attribute this effect to nonspecific interactions between the end of the DNA and the histone proteins removed from the disrupted nucleosome. For those traces, only the naked DNA preceding a nucleosome can be used for correlation, which may result in somewhat lower precision.

Figure 2.4 is an example of the application of this method to a nucleosome unzipping trace. The correlation was performed using two regions of naked DNA flanking the nucleosome (Fig. 2.4A). The generalized correlation function (Fig. 2.4B) shows a maximum of 0.80 at $j_0=-14$ bp and $a=0.93$.

5. DETERMINATION OF UNZIPPING ACCURACY AND PRECISION

To characterize the ability of the unzipping technique to locate the absolute position of an interaction, we unzip naked DNA templates capped with hairpins at distal ends (Fig. 2.5A) and analyze the measured locations of

Author's personal copy

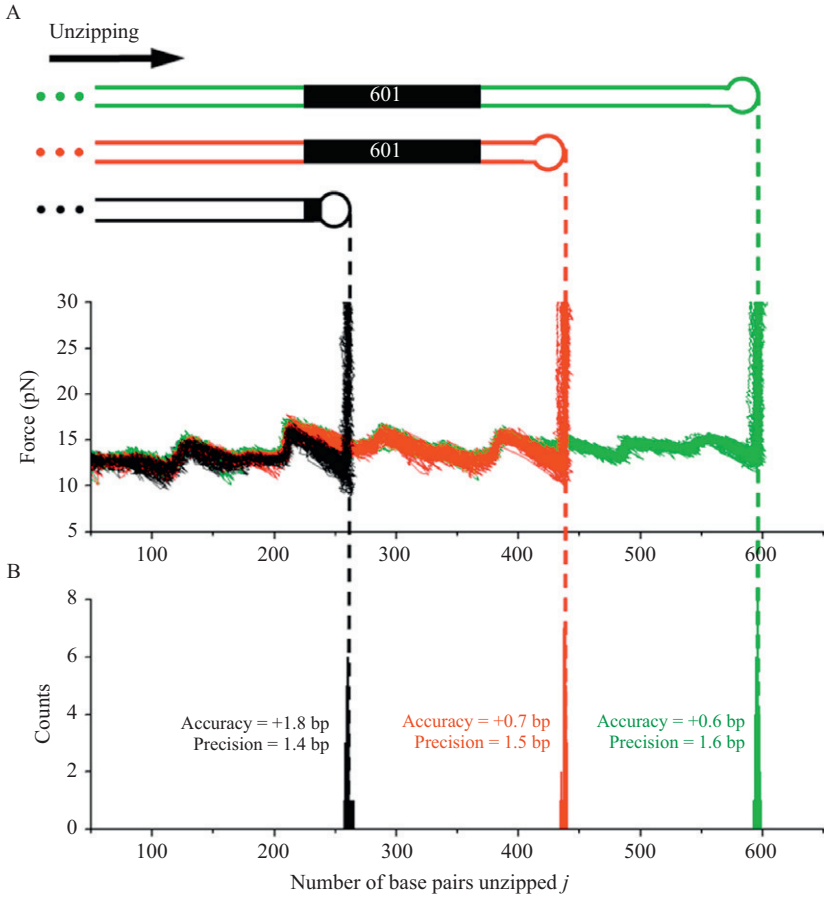


Figure 2.5 Characterization of the accuracy, and precision, of the unzipping method. (Adapted from Hall et al., 2009, with permission from the publisher.) (A) Three hairpin-capped unzipping templates were unzipped using a loading rate clamp (8 pN/s): 258 bp (black, 21 traces), 437 bp (red, 27 traces), and 595 bp (green, 33 traces). (B) For each template, a histogram was generated from the data points in the vertically rising section only. The measured hairpin location of each template was taken as the mean of the histogram. The accuracy was determined by the difference between the mean of the histogram and the expected value (dashed vertical line). The precision was determined by the standard deviation of the histogram.

hairpins (Hall et al., 2009). These hairpins mimic strong binding sites at well-defined locations on DNA. As shown in Fig. 2.5A, three unzipping templates of varying length, each with a hairpin located near where a nucleosome could be assembled, are unzipped. Each unzipping curve follows that

Author's personal copy

of the naked DNA until it reaches the hairpin where the force rises sharply, providing a clear indication of the hairpin location. These unzipping curves are aligned as described above. Figure 2.5B shows histograms of the detected binding locations for each hairpin template and a comparison with expected locations. Note that accuracy is a measure of the closeness of the measured value with the true value, whereas precision is a measure of the repeatability of measurements. For each template, accuracy is given by the difference between the mean measured location and the expected location, while precision is given by the standard deviation of the histogram. For all three templates, the accuracy is within 1 bp and the precision is within 2 bp. Therefore, we conclude that the unzipping technique has the capability to determine the absolute sequence position of an interaction with near single base pair accuracy and precision.

6. UNZIPPING IN NUCLEOSOME STUDIES

Unzipping is ideally suited for the manipulation of protein–DNA interactions and the detection of their dynamics at the single-molecule level. Below, we provide a very brief summary of various studies on nucleosome structure, positioning, and remodeling which we have explored using our unzipping technique. For more specific details regarding these experiments or data analysis, we refer the reader to the original publications (Dechassa et al., 2011; Hall et al., 2009; Jin et al., 2010; Shundrovsky et al., 2006).

6.1. Nucleosome unzipping signature

A nucleosome has the most distinctive signature when unzipped with a loading rate clamp. As an example, we have unzipped a DNA containing a positioned nucleosome in both forward and reverse directions (Dechassa et al., 2011; Hall et al., 2009). In either direction, two regions of strong interactions are detected: one preceding the dyad and one near the dyad (Fig. 2.6C). When results from both directions are combined, the unzipping force signatures reveal three distinct regions of interactions: one located around the dyad axis and the other two $\sim$40 bp on either side of the dyad axis. Within each region, interactions are discretely spaced with $\sim$5 bp periodicity (Fig. 2.6B). By comparison with the crystal structure of the nucleosome, the dyad region should correspond to contacts from the $(H3/H4)_2$ tetramer at superhelical location (SHL) -2.5 to $+2.5$, and the two off-dyad regions should correspond to contacts from the two H2A/H2B dimers between SHL -3.5 to -6.5 and $+3.5$

Author's personal copy

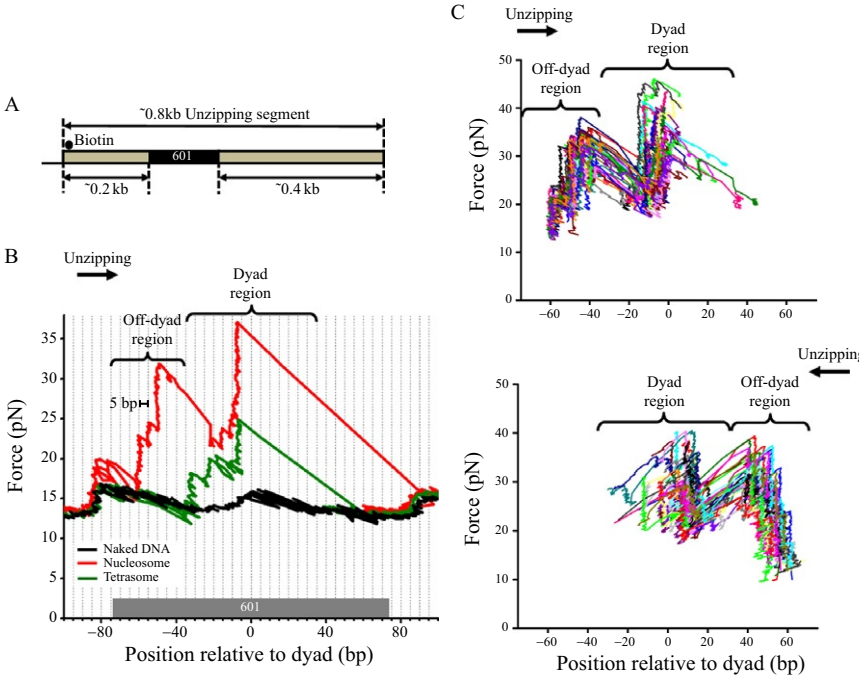


Figure 2.6 Unzipping through a positioned nucleosome using a loading rate clamp at 8 pN/s. (Adapted from Dechassa et al., 2011, with permission from the publisher.) (A) A sketch of the forward nucleosome unzipping segment. (B) Representative force unzipping signatures of naked DNA (black), DNA containing a nucleosome (red), and DNA containing a tetrasome (green). Both the nucleosome and the tetrasome were assembled onto an unzipping segment containing the 601 positioning element. The arrow indicates the unzipping direction. Two distinct regions of interactions, as well as a 5-bp periodicity within each region, were observed for the nucleosome. The tetrasome signature exhibits only a single region of interactions, which substantially overlaps the dyad region identified in the nucleosome. (C) Multiple traces of unzipping through a nucleosome from both forward (upper panel, 31 traces) and reverse (lower panel, 28 traces) directions. Each color represents data obtained from a single nucleosomal DNA molecule. Distinct regions of interactions and a 5-bp periodicity within each region are highly reproducible.

to +6.5, respectively. The absence of the last region for each direction of unzipping also indicates that after the first and second regions are disrupted, the nucleosome structure likely becomes unstable and histone dissociation occurs before the last region can be probed. These features are further discussed below.

Author's personal copy

We have also verified that the unzipping method could clearly distinguish a nucleosome from a tetrasome consisting only of a $(H3/H4)_2$ tetramer (Fig. 2.6B). Unzipping through a tetrasome exhibits only a single region of strong interactions near the dyad and this region substantially overlaps with the dyad region of interactions for canonical nucleosomes (Dechassa et al., 2011).

The nucleosome unzipping signature characteristic of a positioned nucleosome is also shared by nucleosomes on arbitrary sequences (Hall et al., 2009). This was demonstrated by assembling nucleosomes onto a DNA segment that does not contain any known positioning elements (Fig. 2.7A). The assembly condition was controlled to achieve a relatively low saturation level so that each DNA molecule had at most one nucleosome. When such nucleosomal DNA molecules were unzipped with a loading rate clamp using the same conditions as those of Fig. 2.6, nucleosomes were found at various locations on the template (Fig. 2.7B), likely due to a lack of known nucleosome positioning elements on this DNA sequence. Each unzipping trace contains two major regions of strong interaction, with the second region presumably located near the dyad. These nucleosome unzipping signatures possessed essentially identical characteristics to those of the 601 sequence, except that their peak forces within each region were typically smaller by a few pN, reflecting weaker interactions of histone with nonpositioning DNA sequences. The key features remained essentially identical: the three regions of strong interactions with the strongest at the dyad, the 5 bp periodicity, and the loss of nucleosome stability upon dyad disruption (Fig. 2.7B and C).

6.2. High-resolution mapping of histone–DNA interactions in a nucleosome

To quantitatively assay the strengths of the histone–DNA interactions, we unzipped through individual nucleosomal DNA molecules with a constant unzipping force (Hall et al., 2009). Under a force clamp (Johnson, Bai, Smith, Patel, & Wang, 2007), the dwell times at different sequence positions measure the strengths of interactions at those positions. Thus this method allows direct mapping of the strengths of interactions. Figure 2.8A shows example traces for unzipping DNA through a nucleosome under a constant force. DNA molecules were unzipped from both directions along the DNA. In both cases, the unzipping fork did not move through the nucleosomal DNA at a constant rate but instead dwelled at specific locations within the nucleosome, indicating the presence of strong interactions. In particular,

Author's personal copy

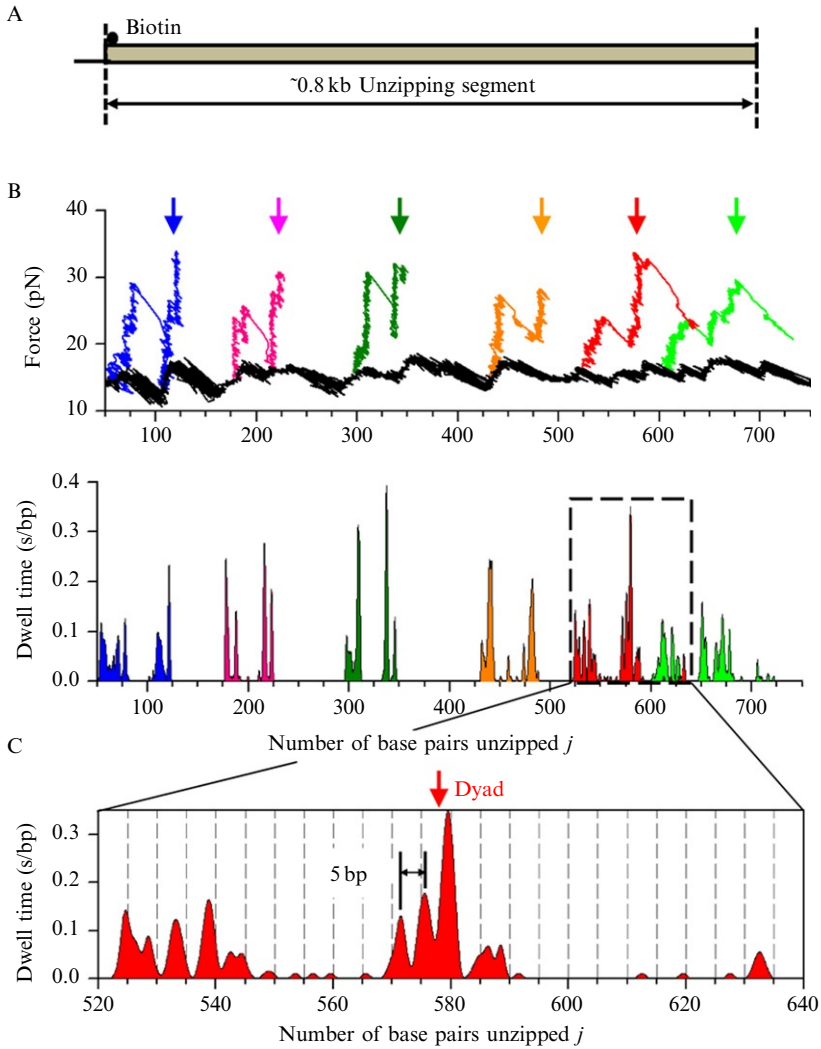


Figure 2.7 Unzipping through a nucleosomes on an arbitrary sequence using a loading rate clamp at 8 pN/s. (Adapted from Hall et al., 2009, with permission from the publisher.) (A) A sketch of the unzipping segment. (B) Force unzipping signature of a nucleosome at different locations on a DNA template lacking known strong positioning elements. Each color was obtained from a single nucleosome unzipping trace, with the unzipping force shown in the top panel and the corresponding dwell time histogram shown in the bottom panel. The unzipping signature of a naked DNA molecule of the same sequence is also shown (black), as a reference. Vertical arrows indicate the observed dyad locations of these nucleosomes. (C) Close-up of the dwell time histogram for a specific unzipping trace (red) to emphasize the 5-bp periodicity observed in each interaction region of the unzipping signature.

Author's personal copy

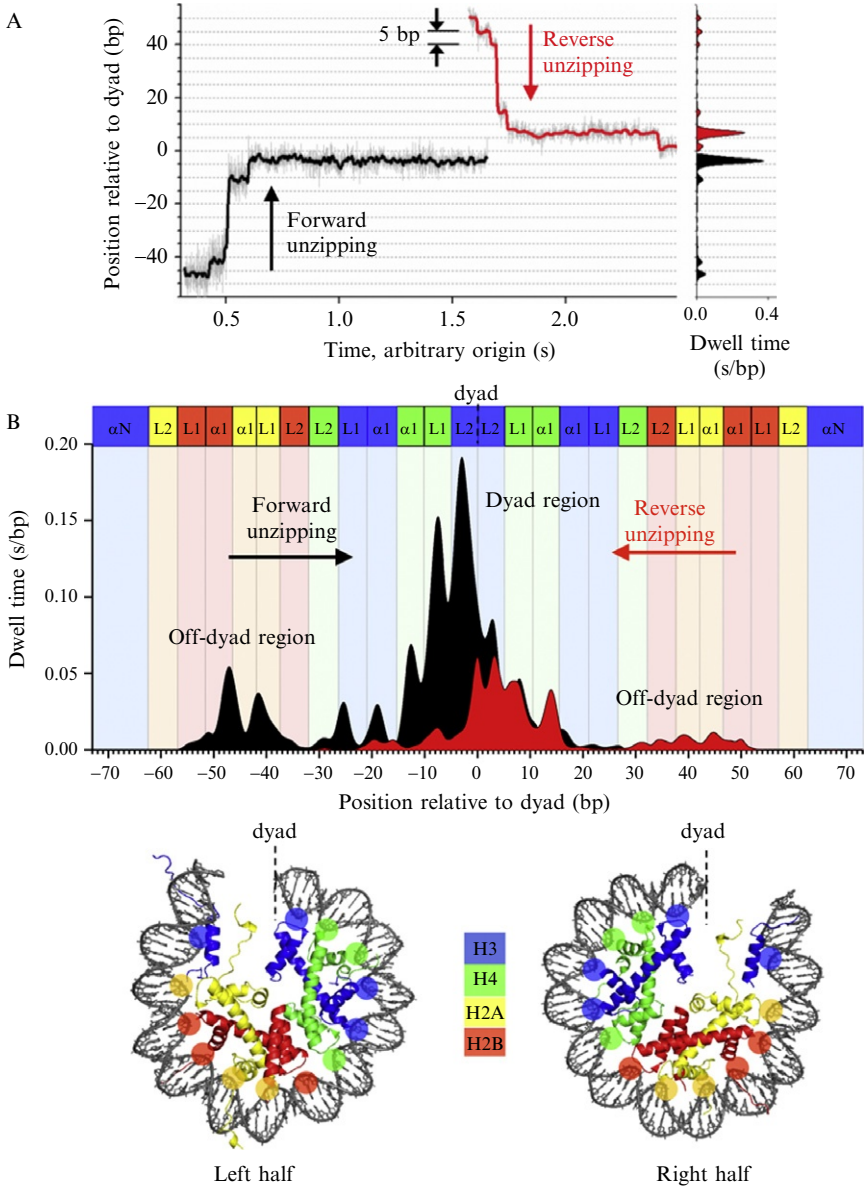


Figure 2.8 Unzipping through a positioned nucleosome using a force clamp at 28 pN. (Adapted from Hall et al., 2009, with permission from the publisher.) (A) Representative traces of forward (black) and reverse (red) unzipping through a nucleosome under a constant applied force (~ 28 pN). The unzipping fork paused at specific locations when passing through a nucleosome, which are evident from both the traces (left) and their corresponding dwell time histograms (right). (B) A histone–DNA interaction map is

Author's personal copy

these traces revealed that the fork dwelled with discrete steps spaced by ~5 bp and the longest dwell times tended to occur near the dyad.

An interaction map was generated by averaging dwell time histogram measurements from many traces from both forward and reverse unzipping, as shown in Fig. 2.8B. Several features, consistent with findings using the loading rate clamp, are evident from these plots:

(1) Histone–DNA interactions are highly nonuniform within a nucleosome. There are three broad regions of strong interactions: one located at the dyad and two ~±40 bp from the dyad. The locations of all three regions are strongly correlated with those estimated from the crystal structure of the nucleosome (Davey, Sargent, Luger, Maeder, & Richmond, 2002; Luger et al., 1997). The locations of these interactions are also consistent with estimates from our nucleosome stretching experiments (Brower-Toland et al., 2002, 2005; Brower-Toland & Wang, 2004), although results from those studies are less direct in identifying the absolute locations of strong interactions and are more difficult to interpret.

(2) An ~5 bp periodicity occurs within each region of interaction. According to the crystal structure of the nucleosome, histone core domains are expected to make strong contacts with the DNA minor groove every 10 bp (Davey et al., 2002; Luger et al., 1997). The observed 5 bp periodicity demonstrated that two distinct interactions at each minor groove contact, one from each strand, could be disrupted sequentially rather than simultaneously.

(3) The interactions near the entry and exit DNA are particularly weak. The unzipping fork did not dwell at a 20-bp region of both entry and exit DNA, indicating that the histones are only loosely bound to the DNA. Note that these weaker interactions are detected by the loading rate clamp described above.

constructed by using a total of 27 traces from the forward direction and 30 traces from the reverse direction. Each peak corresponds to an individual histone–DNA interaction and the heights are indicative of their relative strengths. Three regions of strong interactions are indicated: one located at the dyad and two located off-dyad. The bottom panel is the crystal structure of the nucleosome core particle (Luger et al., 1997), where dots indicate individual histone binding motifs that are expected to interact with DNA. The two halves of the nucleosome are shown separately for clarity. On the top panel, these predicted interactions are shown as colored boxes.

Author's personal copy

(4) For unzipping in both the forward and reverse directions, the first two regions of interactions encountered were always detected, but not the last region. This indicates that once the dyad region of interactions was disrupted, the nucleosome became unstable and histones dissociated from the 601 sequence.

(5) The total dwell time in the nucleosome was longer in the forward direction compared with that in the reverse direction, indicating that nucleosomes were more difficult to disrupt when unzipped in the forward direction, likely reflecting the nonpalindromic nature of the 601 sequence.

These mechanical unzipping experiments resemble the action of RNA polymerase which opens up a transcription bubble and unzips the downstream DNA while advancing into a nucleosome. The histone–DNA interaction map has significant implications for how RNA polymerases or other motor proteins may gain access to DNA associated with a nucleosome (Hall et al., 2009; Jin et al., 2010).

6.3. Nucleosome remodeling

We have also applied the nucleosome unzipping method to investigate nucleosome remodeling dynamics (Shundrovsky et al., 2006). A major advantage of this method is its ability to accurately locate a nucleosome on a long DNA template such that undesired effects of close proximity to DNA ends may be minimized. We have used the unzipping technique to probe the structure of individual nucleosomes after SWI/SNF remodeling. A mononucleosome was initially positioned by 601 in the middle of an ~800-bp unzipping segment (Fig. 2.9A) and was remodeled by yeast SWI/SNF. We used a loading rate clamp to detect the nucleosome after remodeling. For convenience, we defined the nucleosome position simply as the mean location of the off-dyad region. The precision of this method for nucleosome position determination was 2.6 bp, calculated by fitting a Gaussian function to the position histogram of nucleosomes assembled onto the 601 sequence (Fig. 2.9B and C). This precision is somewhat lower than that for the detection of a hairpin because determining a nucleosome position requires the consideration of multiple histone–DNA interaction peaks that vary in amplitude from trace-to-trace due to the nature of a thermally activated disruption process.

We observed that under our experimental conditions SWI/SNF remodeling does not alter the overall nucleosome structure: the histone octamer

Author's personal copy

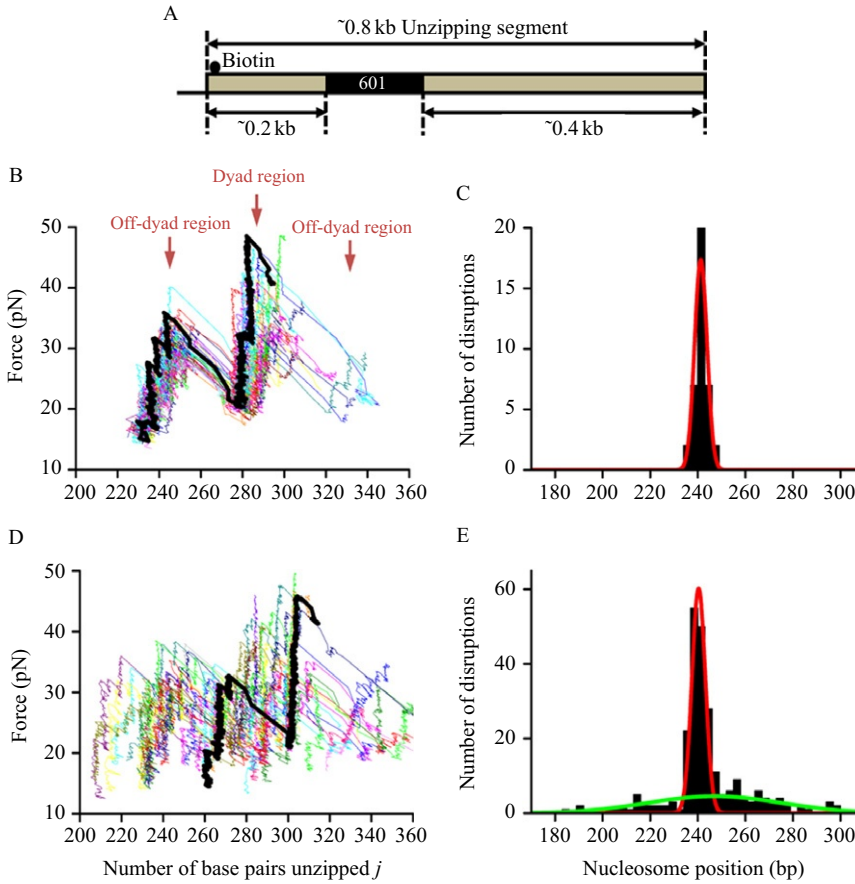


Figure 2.9 Unzipping through nucleosomes before and after remodeling. (Adapted from Shundrovsky et al., 2006, with permission from the publisher.) (A) A sketch of the nucleosome unzipping segment. (B) Unzipping signatures for 30 unremodeled data curves. A single representative curve is highlighted in black. (C) Histogram of unremodeled nucleosome positions on the DNA. A nucleosome position is defined as the mean position of interaction of the first off-dyad region. Data (black) and their Gaussian fit (red) are shown. The distribution is centered at 241 bp, on this particular template, with a standard deviation (SD) of 2.6 bp. (D) Force unzipping signature for 30 data curves obtained after SWI/SNF remodeling. A single representative curve is highlighted in black. (E) Histogram of remodeled nucleosome positions on the DNA after remodeling reaction times <1 min. Data (black) and their fit to two Gaussians (red and green) are shown. The red fit curve represents the nucleosome population that remained at the original 601 position (unremodeled; center $=240$ bp, SD $=2.8$ bp), while the green curve corresponds to those moved by the action of yeast SWI/SNF (remodeled; center $=247$ bp, SD $=28$ bp).

Author's personal copy

remains intact and the overall strength and position of histone–DNA interactions within the nucleosome are essentially unchanged. However, nucleosomes were moved bidirectionally along the DNA with a characteristic spreading of 28 bp per remodeling event (Fig. 2.9D and E). Taken together, these results on SWI/SNF mediated nucleosome remodeling generated by unzipping provide direct measurements of the structure and location of remodeled nucleosomes.

7. CONCLUSIONS

An increasing interest in the nucleosome as a key regulator of chromatin structure and many cellular processes has inspired the development of a variety of novel techniques, particularly at the single-molecule level (for a recent review, see Killian et al., 2012). The unzipping method detailed here offers high accuracy and precision in locating a nucleosome as well as the ability to elucidate both structural and dynamic features of protein–DNA interactions, complementing more traditional techniques. We anticipate that the unzipping method will continue to play an important role in the study of nucleosome structure, regulation, and remodeling and is readily extendable to studies of a wide variety of DNA-based activities.

ACKNOWLEDGMENTS

We thank Dr. Shanna M. Fellman, Dr. Robert A. Forties, Dr. Robert M. Fulbright, James T. Inman, Jessie L. Killian, and Maxim Y. Sheinin for critical comments on the manuscript. We wish to acknowledge support from National Institutes of Health grants (GM059849 to M. D. W.) and National Science Foundation grant (MCB-0820293 to M. D. W.).

REFERENCES

Andrews, A. J., & Luger, K. (2011). Nucleosome structure(s) and stability: Variations on a theme. *Annual Review of Biophysics*, *40*, 99–117.

Ashkin, A., Dziedzic, J. M., Bjorkholm, J. E., & Chu, S. (1986). Observation of a single-beam gradient force optical trap for dielectric particles. *Optics Letters*, *11*, 288.

Bannister, A. J., & Kouzarides, T. (2011). Regulation of chromatin by histone modifications. *Cell Research*, *21*, 381–395.

Bell, O., Tiwari, V. K., Thoma, N. H., & Schubeler, D. (2011). Determinants and dynamics of genome accessibility. *Nature Reviews Genetics*, *12*, 554–564.

Bockelmann, U., Essevaz-Roulet, B., & Heslot, F. (1998). DNA strand separation studied by single molecule force measurements. *Physical Review E*, *58*, 2386–2394.

Bowman, G. D. (2010). Mechanisms of ATP-dependent nucleosome sliding. *Current Opinion in Structural Biology*, *20*, 73–81.

Brower-Toland, B. D., Smith, C. L., Yeh, R. C., Lis, J. T., Peterson, C. L., & Wang, M. D. (2002). Mechanical disruption of individual nucleosomes reveals a reversible multistage

Author's personal copy

release of DNA. *Proceedings of the National Academy of Sciences of the United States of America*, *99*, 1960–1965.

Brower-Toland, B., Wacker, D. A., Fulbright, R. M., Lis, J. T., Kraus, W. L., & Wang, M. D. (2005). Specific contributions of histone tails and their acetylation to the mechanical stability of nucleosomes. *Journal of Molecular Biology*, *346*, 135–146.

Brower-Toland, B., & Wang, M. D. (2004). Use of optical trapping techniques to study single-nucleosome dynamics. *Methods in Enzymology*, *376*, 62–72.

Campos, E. I., & Reinberg, D. (2009). Histones: Annotating chromatin. *Annual Review of Genetics*, *43*, 559–599.

Clapier, C. R., & Cairns, B. R. (2009). The biology of chromatin remodeling complexes. *Annual Review of Biochemistry*, *78*, 273–304.

Das, C., Tyler, J. K., & Churchill, M. E. (2010). The histone shuffle: Histone chaperones in an energetic dance. *Trends in Biochemical Sciences*, *35*, 476–489.

Davey, C. A., Sargent, D. F., Luger, K., Maeder, A. W., & Richmond, T. J. (2002). Solvent mediated interactions in the structure of the nucleosome core particle at 1.9 a resolution. *Journal of Molecular Biology*, *319*, 1097–1113.

Dechassa, M. L., Wyns, K., Li, M., Hall, M. A., Wang, M. D., & Luger, K. (2011). Structure and Scm3-mediated assembly of budding yeast centromeric nucleosomes. *Nature Communications*, *2*, 313.

Dyer, P. N., Edayathumangalam, R. S., White, C. L., Bao, Y., Chakravarthy, S., & Muthurajan, U. M. (2004). Reconstitution of nucleosome core particles from recombinant histones and DNA. *Methods in Enzymology*, *375*, 23–44.

Evans, E. (2001). Probing the relation between force—lifetime—and chemistry in single molecular bonds. *Annual Review of Biophysics and Biomolecular Structure*, *30*, 105–128.

Forties, R. A., North, J. A., Javaid, S., Tabbaa, O. P., Fishel, R., Poirier, M. G., et al. (2011). A quantitative model of nucleosome dynamics. *Nucleic Acids Research*, *39*, 8306–8313.

Fyodorov, D. V., & Kadonaga, J. T. (2003). Chromatin assembly in vitro with purified recombinant ACF and NAP-1. *Methods in Enzymology*, *371*, 499–515.

Gansen, A., Hauger, F., Toth, K., & Langowski, J. (2007). Single-pair fluorescence resonance energy transfer of nucleosomes in free diffusion: Optimizing stability and resolution of subpopulations. *Analytical Biochemistry*, *368*, 193–204.

Gemmen, G. J., Sim, R., Haushalter, K. A., Ke, P. C., Kadonaga, J. T., & Smith, D. E. (2005). Forced unraveling of nucleosomes assembled on heterogeneous DNA using core histones, NAP-1, and ACF. *Journal of Molecular Biology*, *351*, 89–99.

Hall, M. A., Shundrovsky, A., Bai, L., Fulbright, R. M., Lis, J. T., & Wang, M. D. (2009). High-resolution dynamic mapping of histone-DNA interactions in a nucleosome. *Nature Structural & Molecular Biology*, *16*, 124–129.

Jiang, J., Bai, L., Surtees, J. A., Gemici, Z., Wang, M. D., & Alani, E. (2005). Detection of high-affinity and sliding clamp modes for MSH2-MSH6 by single-molecule unzipping force analysis. *Molecular Cell*, *20*, 771–781.

Jin, J., Bai, L., Johnson, D. S., Fulbright, R. M., Kireeva, M. L., Kashlev, M., et al. (2010). Synergistic action of RNA polymerases in overcoming the nucleosomal barrier. *Nature Structural & Molecular Biology*, *17*, 745–752.

Johnson, D. S., Bai, L., Smith, B. Y., Patel, S. S., & Wang, M. D. (2007). Single-molecule studies reveal dynamics of DNA unwinding by the ring-shaped T7 helicase. *Cell*, *129*, 1299–1309.

Joo, C., Balci, H., Ishitsuka, Y., Buranachai, C., & Ha, T. (2008). Advances in single-molecule fluorescence methods for molecular biology. *Annual Review of Biochemistry*, *77*, 51–76.

Kaplan, N., Moore, I. K., Fondufe-Mittendorf, Y., Gossett, A. J., Tillo, D., Field, Y., et al. (2009). The DNA-encoded nucleosome organization of a eukaryotic genome. *Nature*, *458*, 362–366.

Author's personal copy

Killian, J. L., Li, M., Sheinin, M. Y., & Wang, M. D. (2012). Recent advances in single molecule studies of nucleosomes. *Current Opinion in Structural Biology*, *22*, 80–87.

Koch, S. J., Shundrovsky, A., Jantzen, B. C., & Wang, M. D. (2002). Probing protein-DNA interactions by unzipping a single DNA double helix. *Biophysical Journal*, *83*, 1098–1105.

Koch, S. J., & Wang, M. D. (2003). Dynamic force spectroscopy of protein-DNA interactions by unzipping DNA. *Physical Review Letters*, *91*, 028103.

Korber, P., & Becker, P. B. (2010). Nucleosome dynamics and epigenetic stability. *Essays in Biochemistry*, *48*, 63–74.

Lowary, P. T., & Widom, J. (1998). New DNA sequence rules for high affinity binding to histone octamer and sequence-directed nucleosome positioning. *Journal of Molecular Biology*, *276*, 19–42.

Luger, K., Mader, A. W., Richmond, R. K., Sargent, D. F., & Richmond, T. J. (1997). Crystal structure of the nucleosome core particle at 2.8 A resolution. *Nature*, *389*, 251–260.

Luger, K., Rechsteiner, T. J., & Richmond, T. J. (1999). Preparation of nucleosome core particle from recombinant histones. *Methods in Enzymology*, *304*, 3–19.

Mihardja, S., Spakowitz, A. J., Zhang, Y., & Bustamante, C. (2006). Effect of force on mononucleosomal dynamics. *Proceedings of the National Academy of Sciences of the United States of America*, *103*, 15871–15876.

Moffitt, J. R., Chemla, Y. R., Smith, S. B., & Bustamante, C. (2008). Recent advances in optical tweezers. *Annual Review of Biochemistry*, 77, 205–228.

Park, Y. J., & Luger, K. (2008). Histone chaperones in nucleosome eviction and histone exchange. *Current Opinion in Structural Biology*, *18*, 282–289.

Ransom, M., Dennehey, B. K., & Tyler, J. K. (2010). Chaperoning histones during DNA replication and repair. *Cell*, *140*, 183–195.

Ray-Gallet, D., & Almouzni, G. (2010). Nucleosome dynamics and histone variants. *Essays in Biochemistry*, *48*, 75–87.

Schafer, D. A., Gelles, J., Sheetz, M. P., & Landick, R. (1991). Transcription by single molecules of RNA polymerase observed by light microscopy. *Nature*, *352*, 444–448.

Shundrovsky, A., Smith, C. L., Lis, J. T., Peterson, C. L., & Wang, M. D. (2006). Probing SWI/SNF remodeling of the nucleosome by unzipping single DNA molecules. *Nature Structural & Molecular Biology*, *13*, 549–554.

Simon, M., North, J. A., Shimko, J. C., Forties, R. A., Ferdinand, M. B., Manohar, M., et al. (2011). Histone fold modifications control nucleosome unwrapping and disassembly. *Proceedings of the National Academy of Sciences of the United States of America*, *108*, 12711–12716.

Smith, S. B., Cui, Y., & Bustamante, C. (1996). Overstretching B-DNA: The elastic response of individual double-stranded and single-stranded DNA molecules. *Science*, *271*, 795–799.

Thastrom, A., Lowary, P. T., & Widom, J. (2004). Measurement of histone-DNA interaction free energy in nucleosomes. *Methods*, *33*, 33–44.

Wang, M. D., Yin, H., Landick, R., Gelles, J., & Block, S. M. (1997). Stretching DNA with optical tweezers. *Biophysical Journal*, *72*, 1335–1346.

Zhang, Y., Moqtaderi, Z., Rattner, B. P., Euskirchen, G., Snyder, M., Kadonaga, J. T., et al. (2009). Intrinsic histone-DNA interactions are not the major determinant of nucleosome positions in vivo. *Nature Structural & Molecular Biology*, *16*, 847–852.